ELectronics EXpress

LETTER

IEICE Electronics Express, Vol.14, No.21, 1–9

# Influence of surface roughness on polarization property in passive millimeter-wave imaging

**Fei Hu**[1,2], **Xinyi Zhang**[1], **Yayun Cheng**[1,2,3a)], **Ying Xiao**[1], **and Mengting Song**[1]

[1] *School of Electronic Information and Communications, Huazhong University of Science and Technology, Wuhan 430074, China*

[2] *National Key Laboratory of Science and Technology on Multi-Spectral Information Processing, Wuhan 430074, China*

[3] *Innovation Institute, Huazhong University of Science and Technology, Wuhan 430074, China*

a) *chengyy915@163.com*

**Abstract:** Polarimetric measurement can gain more object information when compared to traditional methods. Linear polarization ratio (LPR) of the millimeter-wave thermal emission has been presented recently and proved to be effective in material classification. The LPR classification technique can be used for the metal detection in the soil and concrete ground. The roughness has not been considered in analysing LPR properties and it may affect the classification performance. In this paper, we focus on the influence of surface roughness on LPR. By solving scattering problem, the LPR properties of different roughness parameters are investigated. Theoretical calculations indicate that the LPR value decreases with the increasing of surface roughness. In addition, the applicable scope of LPR classification technique to discriminate rough surfaces is discussed.

**Keywords:** millimeter-wave, passive imaging, polarimetric measurement, rough surface, linear polarization ratio, material classification

**Classification:** Electromagnetic theory

## References

[1] L. Yujiri, *et al.*: "Passive millimeter wave imaging," IEEE Microw. Mag. **4** (2003) 39 (DOI: 10.1109/MMW.2003.1237476).

[2] R. Appleby and H. B. Wallace: "Standoff detection of weapons and contraband in the 100 GHz to 1 THz region," IEEE Trans. Antennas Propag. **55** (2007) 2944 (DOI: 10.1109/TAP.2007.908543).

[3] J. S. Tyo, *et al.*: "Review of passive imaging polarimetry for remote sensing applications," Appl. Opt. **45** (2006) 5453 (DOI: 10.1364/AO.45.005453).

[4] Y. Cheng, *et al.*: "Linear polarization property and fusion method for target recognition in passive millimeter-wave polarimetric imaging," Electron. Lett. **52** (2016) 1221 (DOI: 10.1049/el.2016.0681).



DOI: 10.1587/elex.14.20171005
Received September 29, 2017
Accepted October 5, 2017
Publicized October 20, 2017
Copyedited November 10, 2017

[5] A. Duric, *et al.*: "The fully polarmetric imaging radiometer SPIRA at 91 GHz," IEEE Trans. Geosci. Remote Sens. **46** (2008) 2323 (DOI: 10.1109/TGRS.2008.917212).
[6] M. W. Hyde, *et al.*: "Material classification of an unknown object using turbulence-degraded polarimetric imagery," IEEE Trans. Geosci. Remote Sens. **49** (2011) 264 (DOI: 10.1109/TGRS.2010.2053547).
[7] F. Hu, *et al.*: "Polarization-based material classification technique using passive millimetre-wave polarimetric imagery," Appl. Opt. **55** (2016) 8690 (DOI: 10.1364/AO.55.008690).
[8] A. Sei, *et al.*: "Polarization ratios anomalies of 3D rough surface scattering as second order effects," IEEE Antennas Propagation Society International Symposium **3** (2001) 726 (DOI: 10.1109/APS.2001.960200).
[9] F. T. Ulaby, *et al.*: *Microwave Remote Sensing: Microwave Remote Sensing Fundamentals and Radiometry* (Addison-Wesley, 1981).
[10] D. A. DiGiovanni, *et al.*: "Surface and volumetric backscattering between 100 GHz and 1.6 THz," Proc. SPIE **9078** (2014) 90780A (DOI: 10.1117/12.2051772).
[11] A. Nashashibi, *et al.*: "Measurement and modeling of the millimeter-wave backscatter response of soil surfaces," IEEE Trans. Geosci. Remote Sens. **34** (1996) 561 (DOI: 10.1109/36.485132).
[12] J. Leader: "The relationship between the Kirchhoff approach and small perturbation analysis in rough surface scattering theory," IEEE Trans. Antennas Propag. **19** (1971) 786 (DOI: 10.1109/TAP.1971.1140044).
[13] T. M. Elfouhaily and C. A. Guerin: "A critical survey of approximate scattering wave theories from random rough surfaces," Waves Random Media **14** (2004) R1 (DOI: 10.1088/0959-7174/14/4/R01).
[14] T. M. Zobeck and C. A. Onstad: "Tillage and rainfall effects on random roughness: A review," Soil Tillage Res. **9** (1987) 1 (DOI: 10.1016/0167-1987(87)90047-X).
[15] P. Bertuzzi, *et al.*: "Testing roughness indices to estimate soil surface roughness changes due to simulated rainfall," Soil Tillage Res. **17** (1990) 87 (DOI: 10.1016/0167-1987(90)90008-2).
[16] Y. Oh, *et al.*: "An empirical model and an inversion technique for radar scattering from bare soil surfaces," IEEE Trans. Geosci. Remote Sens. **30** (1992) 370 (DOI: 10.1109/36.134086).
[17] S. Huang, *et al.*: "Backscattering coefficients coherent reflectivities and emissivities of randomly rough soil surfaces at L-band for SMAP applications based on numerical solutions of Maxwell equations in three-dimensional simulations," IEEE Trans. Geosci. Remote Sens. **48** (2010) 2557 (DOI: 10.1109/TGRS.2010.2040748).
[18] Y. Y. Zhang, *et al.*: "The effective permittivity and roughness parameters inversion by the land backscattering measured data," Chin. J. Radio Sci. **31** (2016) 79.
[19] L. Tsang and J. A. Kong: *Scattering of Electromagnetic waves: Advanced Topics* (Wiley-Interscience, 2001).
[20] J. R. Wang and T. J. Schmugge: "An empirical model for the complex dielectric permittivity of soils as a function of water content," IEEE Trans. Geosci. Remote Sens. **GE-18** (1980) 288 (DOI: 10.1109/TGRS.1980.350304).
[21] J. C. Calvet, *et al.*: "Microwave dielectric properties of a silt-loam at high frequencies," IEEE Trans. Geosci. Remote Sens. **33** (1995) 634 (DOI: 10.1109/36.387579).
[22] K. Sato, *et al.*: "Measurements of reflection characteristics and refractive indices of interior construction materials in millimeter-wave bands," IEEE 45th


DOI: 10.1587/elex.14.20171005
Received September 29, 2017
Accepted October 5, 2017
Publicized October 20, 2017
Copyedited November 10, 2017

Vehicular Technology Conference **1** (1995) 449 (DOI: 10.1109/VETEC.1995.504907).

## 1 Introduction

Passive millimetre-wave (PMMW) imaging has been applied to many fields such as remote sensing and security detection on account of its excellent applicability in all time and penetrability in fog, smoke, clothing and so on [1, 2]. PMMW polarimetric measurement is an active field because it can acquire some additional information that complements the insufficiency of other electromagnetic radiation attributes. By this way, the information we can get includes not only traditional radiation attributes (i.e., intensity and spectrum), but also polarization parameters such as degree of polarization, angle of polarization, degree of linear polarization and so on [3]. Polarization parameters can be used for contrast enhancing in target detection [4], man-made object imaging [5] and material classification [6].

More recently, linear polarization ratio (LPR) has been presented to be a new feature discriminator for material classification, which is effective for distinguishing between metals and dielectrics [7]. Possible applications of LPR classification technique mainly include metal target detection in open scenes such as reconnaissance and surveillance, search and rescue, ground navigation. In the previous work, the LPR properties of several materials are analyzed by using Fresnel equation of smooth surface. However, the measurement results [7] indicate that surface roughness can affect LPR distributions. When material surface is regarded as rough compared to electromagnetic wavelength, scattering should be taken into consideration. Thus, it is necessary to analyze the impact of surface roughness on LPR property.

LPR is the feature parameter in PMMW imaging, which is different from polarization ratio in active radar imaging. The latter one is the ratio of scattering coefficients in a certain direction [8]. The former one is the ratio of orthogonal polarization reflectivities (i.e., the integrations of scattering coefficients in all directions [9]) and characters the thermal emission property in PMMW imaging. Much research has been done on studying the scattering properties of various types of terrain at millimeter-wave bands [10, 11], but the LPR property of rough surface has not yet been studied after LPR is presented, especially the relationship between LPR and roughness parameters.

In this paper, soil and concrete are selected as the typical rough materials in many typical scenes. Because the detection of metal in the soil and concrete ground is the main application of LPR classification technique. The LPR expression of rough surface is deduced by using Kirchhoff approximation (KA) model to solve the scattering parameters. By analyzing the relationship between LPR and roughness parameters, the application scope of LPR classification technique for rough surfaces is discussed.


DOI: 10.1587/elex.14.20171005
Received September 29, 2017
Accepted October 5, 2017
Publicized October 20, 2017
Copyedited November 10, 2017

## 2 Fundamental theories

The LPR classification technique is based on LPR discriminator to distinguish between metal and dielectric materials. LPR is defined by the ratio of orthogonal polarization parameters, which can be written as [7]

$$LPR(\theta_i) = [1 - e_h(\theta_i)]/[1 - e_v(\theta_i)] = r_h(\theta_i)/r_v(\theta_i) \tag{1}$$

where $\theta_i$ is the incident angle, $e_h(\theta_i)$ and $e_v(\theta_i)$ represent the horizontally and vertically polarised emissivity respectively, $r_h(\theta_i)$ and $r_v(\theta_i)$ denote the horizontally and vertically polarized reflectivity respectively.

In the practical application of material classification, the optimal selection range of incident angle is from 60° to 70° (in particular, around 65°). The classification criterion is that the material with $LPR \geq \delta$ represents a dielectric, while $LPR < \delta$ implies a metal ($\delta$ is the LPR threshold). LPR threshold is selected using a simple statistical method used in the previous paper [7]. By analyzing the statistical distribution of LPR image grey value, the LPR threshold is selected by the median of a special LPR range in which the LPR statistical count is the minimum. Specifically, we analyze the statistical distribution in many uniform LPR ranges (i.e., $R_i = [LPR_{mini}, LPR_{maxi}]$, in which $i$ is range number). Consequently, LPR threshold $\delta$ can be selected by

$$\delta = (LPR_{minp} + LPR_{maxp})/2 \tag{2}$$

where $LPR_{minp}$ and $LPR_{maxp}$ are the lower and upper limit of a certain small LPR range (i.e., $R_p = [LPR_{minp}, LPR_{maxp}]$) in which the statistical count of LPR values is the minimum. According to the LPR priori information (LPR characteristics) analyzed in Ref. [7], we require that $R_p \subseteq [1, 3]$.

In this paper, we consider soil and concrete as the typical materials in many typical scenes, e.g., metal detection in airfield ground. For soil and concrete, the surface height distribution function is usually Gaussian [9]. Fig. 1 illustrates a plane wave incident upon a Gaussian random rough surface whose RMS height is $h$ and correlation length is $l$. $\widehat{k}_i$ denotes the incident wave vector and $\widehat{k}_s$ denotes the scattering wave vector. $\mu_0$, $\epsilon_0$ is the dielectric parameter and magnetic permeability of air, $\mu_r$, $\epsilon_r$ is the dielectric parameter and magnetic permeability of the ground. $(\theta_i, \phi_i)$ and $(\theta_s, \phi_s)$ represent the incident and scattering directions in spherical coordinate system.

The reflectivity of rough surface can be given by [9]

$$r_p(\theta_i, \phi_i) = \frac{1}{4\pi cos\theta_i} \int_0^{2\pi} \int_0^{\frac{\pi}{2}} [\sigma^r_{pp}(\theta_i, \phi_i; \theta_s, \phi_s) + \sigma^r_{pq}(\theta_i, \phi_i; \theta_s, \phi_s)] sin\theta_s d\theta_s d\phi_s \tag{3}$$

where $\sigma^r_{pq}$ means the bistatic scattering coefficient, $p$ or $q$ means polarization direction and they are horizontal or vertical polarization ($h$ or $v$). $\sigma^r_{pp}$ means $p = q$ and the bistatic scattering coefficient with the same polarization mode. The general formula to calculate $\sigma^r_{pq}$ can be defined as

$$\sigma^r_{pq} = \frac{4\pi R^2 Re[\langle |E^s_{pq}|^2 \rangle / \eta^*_s]}{A_0 Re[|E_0|^2 / \eta^*_1]} \tag{4}$$

where $A_0$ is the irradiation area and $R$ means the distance of observation point to the center of $A_0$, $E^s_{pq}$ is the electric field intensity of scattering field with different


DOI: 10.1587/elex.14.20171005
Received September 29, 2017
Accepted October 5, 2017
Publicized October 20, 2017
Copyedited November 10, 2017

polarization modes, $\eta$ is intrinsic impedance in the medium, $*$ is complex conjugate symbol. As shown in Fig. 1, incident and scattering both occurs in the region 1 (air), so $\eta_s = \eta_1$. $Re[\cdot]$ is real number operation. The rough surface analyzed in this paper is azimuthally symmetric, so the relationship between the reflectivity and the azimuthal angles ($\phi_i$ and $\phi_s$) can be neglected. We only consider the incident angles ($\theta_i$ and $\theta_s$).

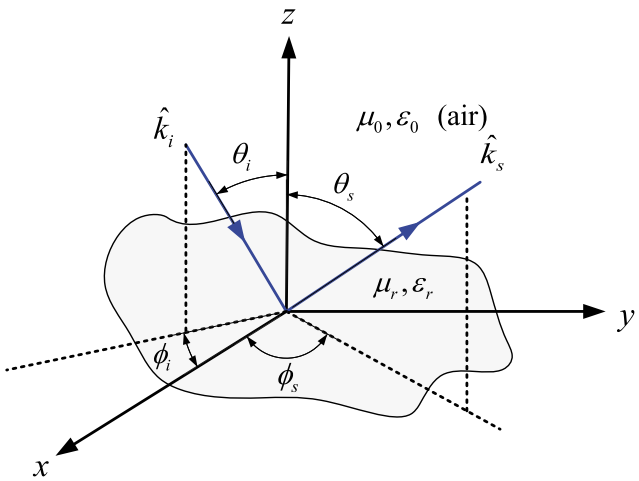


**Fig. 1.** Geometrical configuration of scattering problem

KA model is the widely used method to calculate the scatting parameters of Gaussian random rough surface [12, 13]. The application scope of KA is $kl > 6$ and $l^2 > 2.76h\lambda$ [9], where $k$ is the wavenumber. According the typically measured data of published papers [14, 15, 16, 17, 18], we can obtain the typical roughness scopes of soil and concrete. In this paper, we only analyze these typical kinds of roughness. For soil, the RMS height $h$ ranges from millimeter-level to centimeter-level, and the correlation length $l$ ranges from centimeter-level to decimeter-level. For concrete, the difference of surface roughness is slight in general. The RMS height $h$ ranges around decimillimeter-level, and the correlation length $l$ ranges around centimeter-level. Therefore, KA model is utilized to analyze the scattering problem of soil and concrete at the millimeter-wave band (e.g., W band) in this paper.

The function of horizontal and vertical polarization reflectivity for Gaussian random rough surface has been deduced by Leung Tsang [19]. It can be expressed as

$$\begin{aligned}\begin{pmatrix} r_v(\theta_i) \\ r_h(\theta_i) \end{pmatrix} = \int_0^{\frac{\pi}{2}} d\theta_s sin\theta_s \int_0^{2\pi} d\phi_s \frac{1}{2\pi h^2 |\rho''(0)|} \cdot exp\left[ -\frac{\overline{q}_x^2 + \overline{q}_y^2}{2\overline{q}_z^2 h^2 |\rho''(0)|} \right] \\ \cdot \frac{|\overline{q}|^4}{4cos\theta_i [(\widehat{h}_s \cdot \widehat{k}_i)^2 + (\widehat{v}_s \cdot \widehat{k}_i)^2] \overline{q}_z^4} \\ \cdot \begin{pmatrix} (\widehat{h}_i \cdot \widehat{k}_s)^2 |R_{h0}|^2 + (\widehat{v}_i \cdot \widehat{k}_s)^2 |R_{v0}|^2 \\ (\widehat{v}_i \cdot \widehat{k}_s)^2 |R_{h0}|^2 + (\widehat{h}_i \cdot \widehat{k}_s)^2 |R_{v0}|^2 \end{pmatrix}\end{aligned} \tag{5}$$

where $\rho''(0)$ means the second order derivative of surface auto-covariance at the origin, and it can be expressed that $\rho''(0) = 2/l^2$, $R_{h0}$ and $R_{v0}$ are the Fresnel


DOI: 10.1587/elex.14.20171005
Received September 29, 2017
Accepted October 5, 2017
Publicized October 20, 2017
Copyedited November 10, 2017

reflection coefficient of horizontal and vertical polarization, $\widehat{h}$ and $\widehat{v}$ are the unit vector on the horizontal and vertical polarization direction of electromagnetic wave, $\widehat{k}$ means the unit vector on the propagation direction of electromagnetic wave, $\overline{q}, \overline{q}_x, \overline{q}_y, \overline{q}_z$ are relevant to coordinate systems that derivated by Kirchhoff Stationary-Phase approximation, $\widehat{k}_i, \widehat{k}_s, \widehat{h}_i, \widehat{h}_s, \widehat{v}_i, \widehat{v}_s$ are the unit vectors on the propagation and polarization direction in Cartesian coordinate system.

## 3 Calculated results

According to the equation (1) and (5), the 94 GHz LPRs of soil and concrete surface are calculated. The dielectric parameter of soil with 10% moisture is $\epsilon_r = 4.11 - j\,0.35$ [20, 21], and that of concrete is $\epsilon_r = 6.20 - j\,0.34$ [22]. Fig. 2 illustrates the relationship between incident angle and LPR of different roughness. There is still a difference in LPR between dielectric and metal, even if the roughness is taken into consideration. In addition, it is clear that the roughness has significant effect on LPR. To explain the influence of roughness easily, mean square surface slop is introduced to describe the roughness, which is given by [19]

$$s^2 = 2h^2/l^2 = h^2|\rho''(0)|. \tag{6}$$

We can obtain that LPR decreases with the increase of $s^2$ for the same materials. But all LPRs of rough surface are smaller than that of smooth surface. Each LPR curve has a peak angle. The variation of LPR is due to the difference in the polarization emissivity or reflectivity. As depicted in Fig. 3, the emissivities of soil and concrete at 94 GHz are calculated by KA model and Fresnel equations. The LPR peak difference of soil is more significant than that of concrete. Because soil is usually rougher than concrete in the actual situations and the mean square surface slop $s^2$ of concrete is smaller than that of soil in our theoretical calculations.

For the same materials of different roughness, the difference of Brewster angles is slight. Therefore, there is the approximately equal peak angle for the same materials in Fig. 2. The specific values of Brewster angles and LPR peak angles are listed in Table I and Table II. Two tables indicate that the LPR peak angle is very close to the Brewster angle, especially the concrete. The surface roughness ($s^2$) is smaller, the difference between the LPR peak angle and the Brewster angle is smaller. These phenomenons result from the formula difference between LPR and emissivity. Acorrding to the equation (1), a small $e_h$ and a big $e_v$ can get a big LPR. Brewster angle is the angle with the emissivity peak of vertical polarization ($e_v$), while LPR peak angle is the angle with the LPR peak. From the Fig. 3, $e_h$ decreases with the increasing incident angle, while $e_v$ increases at the beginning and then decreases with the increasing of incident angle. When the incident angle reaches the Brewster angle, the LPR may not reach the peak. Because when the incident angle exceeds the Brewster angle slightly, $e_h$ is smaller than the one at the Brewster angle and the descent rate of $e_h$ is bigger than that of $e_v$. Therefore LPR peak angle is bigger than Brewster angle theoretically. In addition, the scattering of rough surface changes the variation regular of emissivity with incident angle. Then the synthetic effects of $e_h$ and $e_v$ result in the decreasing of Brewster angle and the increasing of LPR peak angle.


DOI: 10.1587/elex.14.20171005
Received September 29, 2017
Accepted October 5, 2017
Publicized October 20, 2017
Copyedited November 10, 2017

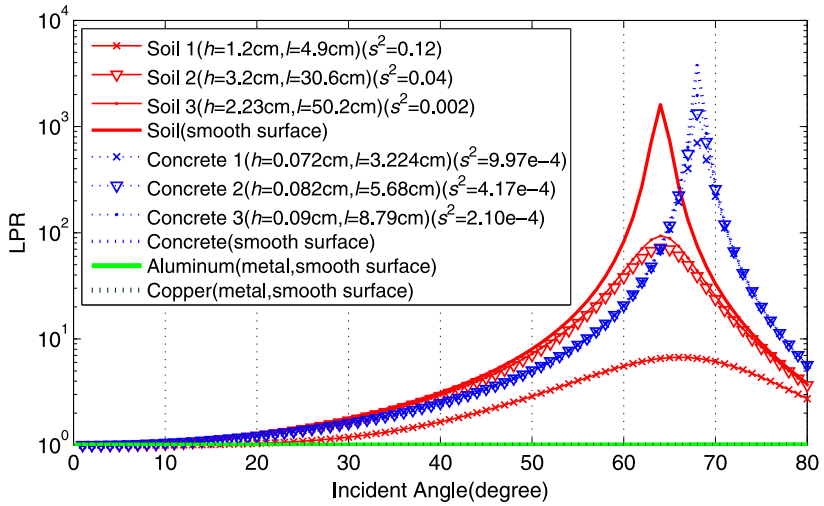


**Fig. 2.** Theoretical LPR of different roughness changing with incident angel at 94 GHz.

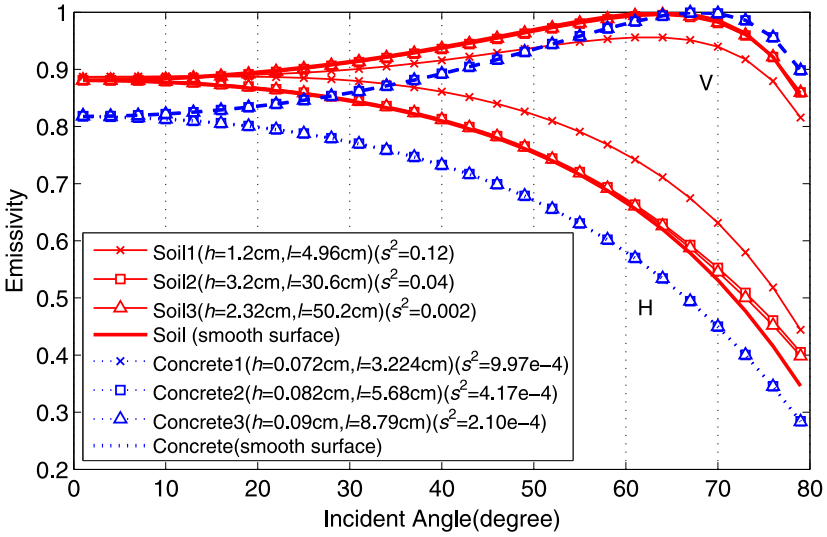


**Fig. 3.** Emissivity of soil and concrete at 94 GHz. H and V denote horizontal and vertical polarization respectively

In order to further study the influence of roughness on LPR, we take $h$ or $l$ as the independent variable to analyze the LPR changing regulations respectively. Due to the similar property, we only take soil as an example in this paper. We select a set of incident angles $[60°, 65°, 70°]$ around the peak angle and choose a suitable scope of $h$ and $l$ in actual situations.

Fig. 4 illustrates the theoretical LPR changing with correlation length at 94 GHz. For each curve of rough surface, LPR is increasing with the rising of correlation length. The horizontal line represents the LPR of smooth surface and it is the upper-bound line of different rough surfaces at the same incident angle. Fig. 5 illustrates the theoretical LPR changing with RMS height at 94 GHz. For each curve of rough surface, LPR is decreasing with the rising of RMS height. The horizontal line represents the LPR of smooth surface and it is also the upper-bound line of different rough surfaces at the same incident angle.


DOI: 10.1587/elex.14.20171005
Received September 29, 2017
Accepted October 5, 2017
Publicized October 20, 2017
Copyedited November 10, 2017

**Table I.** The surface parameters of soil used in the simulations, and the results of peak angles.

| Surface | RMS Height ($h$) | Correlation Length ($l$) | $s^2$ | Brewster Angle | LPR Peak Angle |
|---|---|---|---|---|---|
| Soil (smooth surface) | - | - | - | 64° | 64° |
| Soil 1 | 1.2 cm | 4.96 cm | 0.12 | 62.5° | 66.1° |
| Soil 2 | 3.2 cm | 30.6 cm | 0.04 | 63.8° | 64.3° |
| Soil 3 | 2.32 cm | 50.2 cm | 0.002 | 63.9° | 64.1° |

**Table II.** The surface parameters of concrete used in the simulations, and the results of peak angles.

| Surface | RMS Height ($h$) | Correlation Length ($l$) | $s^2$ | Brewster Angle | LPR Peak Angle |
|---|---|---|---|---|---|
| Concrete (smooth surface) | - | - | - | 68.1° | 68.1° |
| Concrete 1 | 0.072 cm | 3.224 cm | 9.97e-4 | 68.1° | 68.1° |
| Concrete 2 | 0.082 cm | 5.68 cm | 4.17e-4 | 68.1° | 68.1° |
| Concrete 3 | 0.09 cm | 8.72 cm | 2.10e-4 | 68.1° | 68.1° |

In general, with the increasing of $l$ and the decreasing of $h$, the surface is smoother. So, we can draw the conclusion that the surface is smoother, the LPR is larger. But all values are smaller than that of absolutely smooth surface. In order to determine the applicable scope of LPR classification technique to discriminate rough surfaces, the upper limit of surface roughness is discussed. According to the Ref. [7], the selection range $R_p$ of LPR threshold is required that $R_p \subseteq [1, 3]$. So we regard that if the LPR value is less than 3, the LPR classification technique will be not available. As shown in Fig. 6, for soil, if $s^2$ is higher than 0.3, LPR will be less than 3. Specific values of $l$ and $h$ can be calculated by the application scope function of KA. By this way, available ranges of other materials can be also obtained.

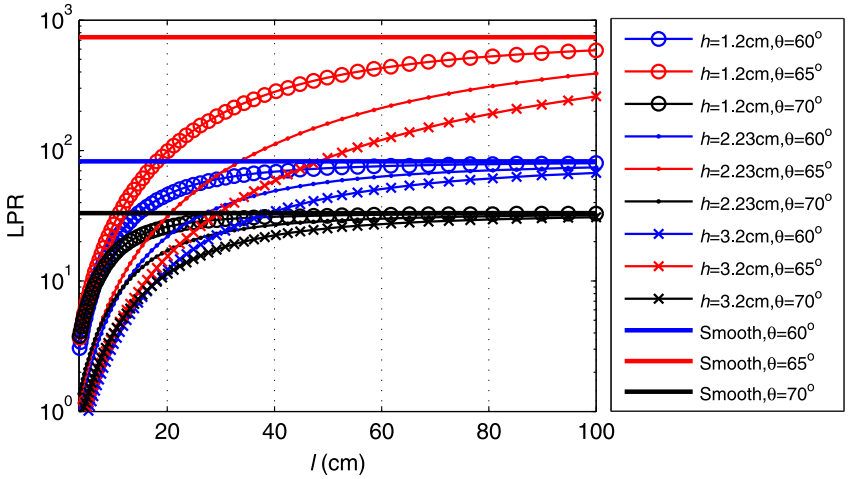


**Fig. 4.** LPR changing with correlation length ($l$)


DOI: 10.1587/elex.14.20171005
Received September 29, 2017
Accepted October 5, 2017
Publicized October 20, 2017
Copyedited November 10, 2017

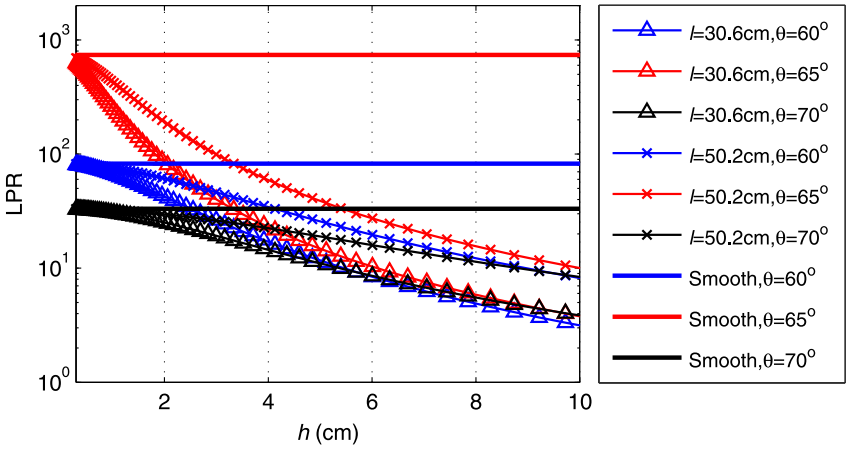


**Fig. 5.** LPR changing with RMS height ($h$)

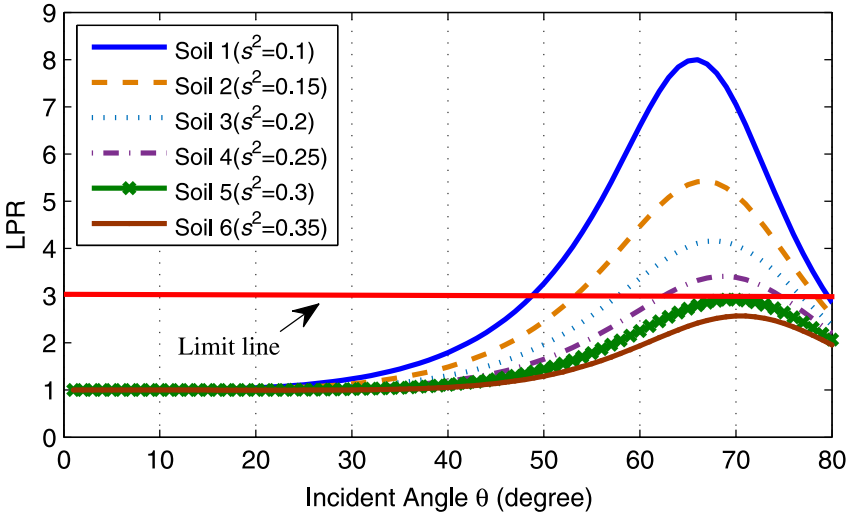


**Fig. 6.** LPR changing with mean square surface slop ($s^2$)

## 4 Conclusion

The LPR classification technique has been presented recently and proved to be effective to distinguish between metals and dielectrics. For the rough surfaces of soil and concrete, we have investigated the influence of roughness parameters on LPR. The calculated results indicate that LPR decreases with the increasing of surface roughness. According to the LPR classification criterion, the upper limit of surface roughness has been obtained. This method can be available for other rough materials. Our work has the guidance meaning for the LPR classification technique, because the surface is usually rough in the practical applications. In the future, the imaging experiments will be carried out to analyse the performance of material classification in various rough surface scenes.

## Acknowledgements

The authors would like to thank the fully support from the Fundamental Research Funds for the Central Universities, HUST under Grant No. 2017JYCXJJ036.


DOI: 10.1587/elex.14.20171005
Received September 29, 2017
Accepted October 5, 2017
Publicized October 20, 2017
Copyedited November 10, 2017